Received: 11 July 2018 | Revised: 4 June 2019 | Accepted: 25 July 2019

DOI: 10.1002/ima.22361

RESEARCH ARTICLE

WILEY

Removal of noise in MRI images using a block difference-based filtering approach

I. Nagarajan[1] | **G.G. Lakshmi Priya**[2]

[1]School of Computer Science and Engineering, VIT, Vellore, India

[2]School of Information Technology and Engineering, VIT, Vellore, India

Correspondence
G.G. Lakshmi Priya, School of Information Technology and Engineering, VIT, Vellore, India
Email: lakshmipriya.gg@vit.ac.in

Abstract

Magnetic resonance imaging (MRI) images are frequently sensitive to certain types of noises and artifacts. The denoising of MRI images is essential for improving visual quality and reliability of the quantitative analysis of diagnosis and treatment. In this article, a new block difference-based filtering method is proposed to denoise the MRI images. First, the normal MRI image is degraded by a certain percentage of noise. The block difference between the intensity of the normal and noisy MRI is computed, and then it is compared with the intensity of the blocks of the normal MRI image. Based on the comparison, the pixel weights are updated to each block of the denoised MRI image. Observational results are brought out on the BrainWeb and BraTS datasets and evaluated by performance metrics such as peak signal-to-noise ratio, structural similarity index measures, universal quality index, and root mean square error. The proposed method outperforms the existing denoising filtering techniques.

KEYWORDS

denoising, filtering, MRI, pixel similarity, Rician noise

1 | INTRODUCTION

The magnetic resonance imaging (MRI) technique is one of the most popularly used imaging techniques for clinical diagnosis and treatment. MRI images are normally involved with low signal-to-noise ratios (SNRs). However, MRI images are degraded by certain noises and artifacts. There are several cases of noise occurrence in MRI images, which include thermal, Gaussian, and Rician noise.[1] These noises create image distortion and blurring, and also complicate the process of pulling up significant data for medical diagnosis. Thus, removing noise in MRI images is essential for better image visualization and promotes reliability of the associated quantitative analysis. The process of denoising the image is a great challenge in the medical area.[2] The best approach to get good quality of MRI images is to average the multiple repeatedly acquired images. Nevertheless, it increases the acquisition time and is not suitable for application where quick methods are required. Nevertheless, practical implementation is not always possible because of the discomfort of patient and limitations of technical aspects. Some other significant aspect of noise is the thermally active electrons in the body of the patient, thus affecting the quality of MRI images. Hence, there is a necessity to develop an efficient method to get rid of the noise in the seized image.

The denoising technique is generally classified into two types, which includes linear and nonlinear filtering techniques.[3] Furthermore, the linear filters are classified as spatial and temporal filters. In the case of linear filters, the noise is reduced by changing the image element value of weighted-mean neighborhood pixels and it creates a poor quality of image.[4] The nonlinear filter is processed within the filter windows. The neighboring pixels are organized along the basis of sample attributes of a windowpane. Consequently, it makes the right character of image.[5] The best solution for diagnosis made is a nonlinear filter rather than a

linear filter as it diminishes the noise as well as keeps the boundaries represented by pixels. The nonlinear denoising methods[6] include a median filter, a bilateral filter, an anisotropic diffusion filter (ADF), and a nonlocal mean filter (NLM).

All the existing filtering methods are focused to remove the noise while keeping fine details and borders of the MRI images. The median filter[7] is also recognized as a benchmark filter, which replaces a pixel by the median, instead of the mean of all pixels in a specified neighborhood. The drawback of the median filter is that it results in causing blurring of an image. Perona and Malik proposed an ADF[8] that applies the law of dispersion on the intensities of the pixels to smooth out textures of the MRI image. A threshold function is applied to prevent diffusion that happens across edges, and thus it preserves the edges in the image. The ADF gives a better output than a median filter. Merely, it has certain limitations such as removing the small features of the image and adds the effect of the staircase to the filtered image.[8] Tomasi and Manduchi proposed a bilateral filter[9] to produce fine edges while keeping fine details and borders of the MR Images. This sets back each pixel intensity with a weighted average of intensity values from the nearby pixels. This weight can be found using the Gaussian distribution. The bilateral filter approach deliberates the gray level and color based on their photometric and geometric similarities. The primary disadvantage of the bilateral filter is that it does not preserve small structures in an image and reject it by taking up as noise.[9]

One of the state-of-the-art methods for denoising MR image is the NLM filter.[10] The NLM filter is introduced as the well-known parameterized filter. The major difference between the NLM filter and other filters is that the NLM filter determines similarity based on the region rather than pixels. It works by creating a weighted mean of the pixels in a relatively large search window and assigns higher weights to pixels with similar neighboring patterns.[11] Finally, the NLM filter reduces the Gaussian-distributed noise. Nevertheless, the Rician or noncentral chi-distribution noise is the generally available noise in the magnitude of MRI, which prevents a nonzero mean and causes bias to actual MRI images when the SNR is low. Many different versions of the NLM filter improved the accuracy of denoising. However, the NLM filter and its version lead to blur high-contrast particles on the MRI images.[12] To improve the visual quality of MRI images, wavelet-based NLM (WBNLM)[13] has been introduced and it exploits the excellent localization property of the wavelet transform while retaining the main coefficients and its neighbors (structures), which might have been shrinking in the conventional wavelet denoising. The structural similarity is manipulated by averaging the current significant coefficient and its neighbors by the NLM filter. So, the structures are retained while the noisy coefficients are averaged out. Thus, the ringing artifacts would be alleviated compared to the conventional wavelet denoising while keeping the structures very well like the spatial domain NLM filter. An iterative bilateral filter[14] is proposed for the noise reduction of MRI images. The filter works by combining gray levels depending on both the geometric closeness and photometric similarity. It removes the adjacent values to distant values in both domain and range. Two weighing functions are designed for spatial and radiometric information, which are designed to modify a pixel value with an average of similar and nearby pixel values in a neighborhood. Recently, it has been proposed that the spatial adaptive nonlocal mean (SANLM)[15] improves the quality of MRI images. The noise level of an image can be eradicated spatially by this method. It can be judged locally by processing data with static or spaciously erratic noise fields in a fully automatic mode. The recent denoising techniques of MRI images are gained from the NLM method, which is the province of art method in the MRI denoising approaches. The main drawback of NLM filter is its computation time. Many research works are carried out for denoising MRI images to increase the peak signal-to-noise ratio (PSNR) value of denoised images and reduce the computation time.

The primary focus of the proposed method is to increase the PSNR value by removing the Rician noise in MRI images based on noise variance. The proposed method deals with assigning weights to the pixels based on the calculation of variance of noise between the noisy image and normal image to enhance the tone of an image. Primarily, the normal image is taken down with certain noise to create the noisy image. And so, both the normal and noise images are partitioned into blocks of equal size. If the block difference (BD) of the noise image and the normal image is equal to zero, the blocks of the denoised image are updated with the normal image block intensity. If the BD is less than zero, the blocks of the denoised image are updated with a value by subtracting the BD from the intensity of the blocks of the noisy image. If the BD of the pixel intensity is larger than zero, the blocks of the denoised image are updated with values by adding the BD from the intensity of the blocks of the noisy image. Thus, in the proposed method, by comparing the pixel intensity of each block of an image, the irrelevant features are identified and removed. The fine structures are preserved carefully for better clinical diagnosis. Hence, the computation time is very less because the blockwise comparison has been utilized.

The proposed method is compared with the state-of-the-art methods such as bilateral, ADF, and NLM for denoising MRI images and also compared with the recent methods

such as IBLF, WBNL, and SANLM. The proposed method produces a convincing result rather than existing filtering techniques. The computation burden is also reduced by the proposed method. The general block diagram of the proposed method is depicted in Figure 1. The research article is organized as follows: Section 2 explains briefly about MRI noise. Section 3 describes the proposed BD-based filtering technique. Section 4 describes the experimental results and discussion. The determination and future work are given in Section 5.

2 | NOISE IN MR IMAGE

The multiplicative or additive noises may occur in MRI images. The primary source of noise in an MRI image is thermal noise.[16] This can be obtained as an additive, white, and Gaussian noise distributed with zero mean and same variance. The MRI is reconstructed by an inverse discrete Fourier (DF) transform. The MRI image has imaginary and real parts affected by Gaussian noise because of linearity and orthogonal principles. The magnitude component of the MRI images is important as it is influenced by the Rician noise distribution. The probability density function (PDF) of the abovementioned noise is performed using Equation (1):

$$f\left(\frac{V_i}{Z}\right)=\frac{V_i}{\sigma^2}\exp\left(-\frac{V_i^2+Z^2}{2\sigma^2}\right)I_n\left(\frac{V_iZ}{\sigma^2}\right), \tag{1}$$

where Z represents the concatenation of the actual and imaginary signal density of the MRI image, V_i represents the measured pixel intensity, and I_n represents the modified null-order Basel function. σ represents noise SD. The SNR of Z/σ has an effect on the structure of Rician distribution. If the SNR value is smaller than the Rician distribution, then it suits a Rayleigh distribution[17] and the PDF is given in Equation (2):

$$f_{\text{magnitude}}(V)\approx\frac{V}{\sigma^2}e^{-\left(\frac{V^2}{2\sigma^2}\right)}. \tag{2}$$

If the SNR is larger, then the Rician distribution becomes a Gaussian distribution and the PDF is given in Equation (3):

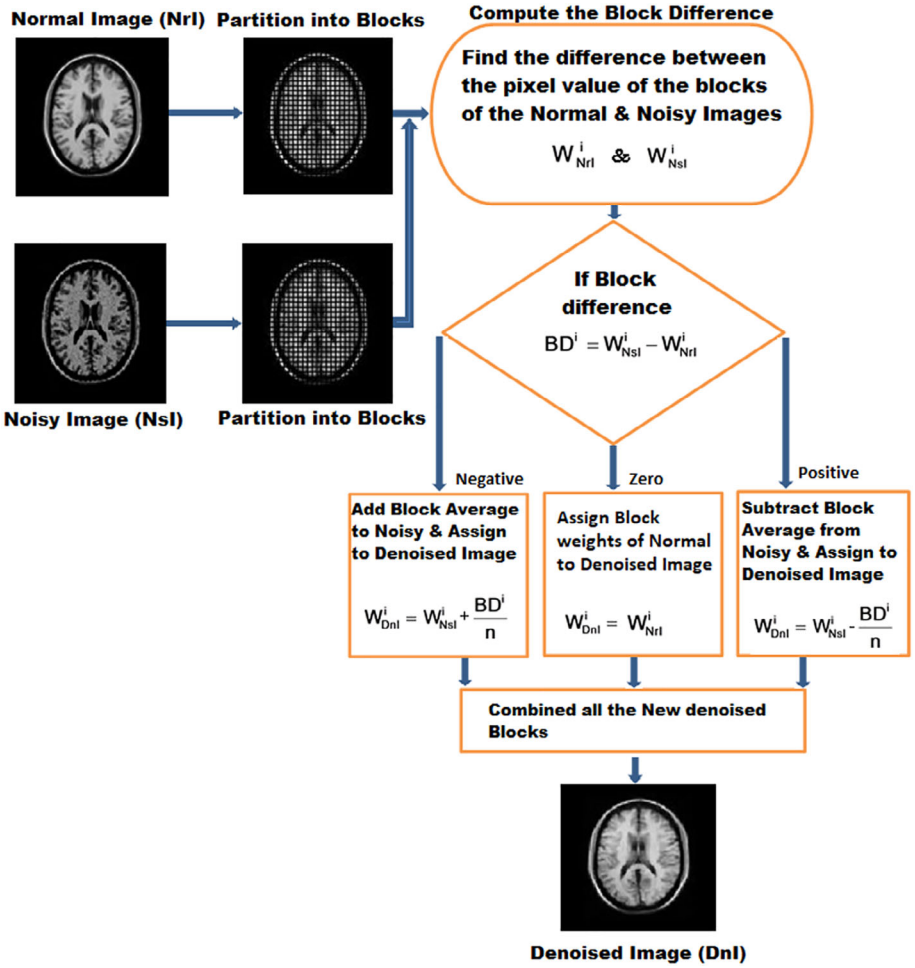

FIGURE 1 The flow diagram of the proposed method [Color figure can be viewed at wileyonlinelibrary.com]

$$f_{\text{magnitude}}(V) \approx \frac{1}{\sqrt{2\pi\sigma^2}} e^{-\left(\frac{V-\sqrt{Z^2+\sigma^2}}{2\sigma^2}\right)}. \quad (3)$$

The Rician noise produces random fluctuation in the MRI image[18] as it can also reduce the contrast of the image. It is signal-oriented noise rather than additive, it also decreases the fine features of MRI images in qualitative and quantitative aspects. Hence, it is very difficult to remove in MRI images. The proposed work focuses on the removal of noise based on the noise variance of each block of the MRI image, so the features are maintained in both qualitative and quantitative manners. The detailed discussion of the proposed work is described in Section 3.

3 | BD-BASED FILTERING METHOD

The noise reduction in MRI images is a real challenging task for a medical practitioner. Various research works are carried out to denoise the MRI images. The proposed method focuses on BD-based comparison and reduction methods of MRI images. First, the normal image was added with a certain percentage of Rician noise (3%-30%). Then the normal image and noisy image are partitioned into fixed size blocks. Each block of the normal image is compared with the corresponding blocks of a noisy image. Based on the comparison, the pixel weights are assigned in the blocks of the denoised image. The detailed explanation of the proposed method is as follows.

Let OB_1, $OB_2 \ldots OB_m$ represent the blocks of the normal image (*NrI*), where m denotes the number of the blocks. *NrI* is represented using Equation (4):

$$NrI = \sum_{i=1}^{n} OB_j^i, \quad (4)$$

where $j = 1, 2 \ldots m$, the number of the blocks OB_1, $OB_2 \ldots OB_m$. OB_j^i is the $i$thpixel value of the jth block of the given image NrI, where $i = 1, 2 \ldots n$, the number of pixels in the jth block of the image *NrI*. A certain percentage (3–30%) of Rician noise is added to the *NrI* to get a noisy image (*NsI*) and it is given in Equation (5):

$$NsI = NrI + \text{Noise}. \quad (5)$$

Let NB_1, $NB_2 \ldots NB_m$ represent the blocks of *NsI*, where m denotes the number of the blocks. *NsI* is represented as Equation (6):

$$NsI = \sum_{i=1}^{n} NB_j^i, \quad (6)$$

where $j = 1, 2 \ldots n$ is the number of blocks of *NsI* and NB_j^i is the ith pixel value of jth block of the image *NsI*.

The BD between each block of the *NrI* and *NsI* is calculated by finding the difference between each pixel value of the blocks of both images. It is computed using Equation (7):

$$BD_j^i = \left(NB_j^i - OB_j^i\right), \quad (7)$$

where BD_j^i represents the BD of the ith pixel of the jth block. The weight of each pixel of the block of the new *DnI* is updated as given below:

Step 1: If the BD between the pixels of the block of *NrI* and *NsI* is zero, then the pixel value of *NrI* can be assigned to the pixels of the block of *DnI* and is represented in Equation (8).
Step 2: If the BD between the pixels of the block of *NrI* and *NsI* is less than the corresponding pixel value of the block of *NrI*, then subtract the average of the BD value from each pixel of the block of *NsI* and assign it to the corresponding pixel of the block of the new *DnI* and is represented in Equation (8).
Step 3: If the BD between the pixels of the block of *NrI* and *NsI* is greater than the corresponding block in *NrI*, then add the average of the BD value from each pixel of the block of *NsI* and assign it to the corresponding pixel of the block of the new *DnI* and is represented in Equation (8).

$$DnI_j^i = \begin{cases} NrI_j^i & \text{if } BD_j^i \text{ is zero} \\ NsI_j^i - \left(BD_j^i \div \text{block size}\right), & \text{if } BD_j^i \text{ is positive} \\ NsI_j^i + \left(BD_j^i \div \text{block size}\right), & \text{if } BD_j^i \text{ is negative} \end{cases} \quad (8)$$

where DnI_j^i represents the weight of ith pixel of the jth block of *DnI*; BD_j^i represents the block difference of the ith pixel of the jth block of the difference image and the block size is 5; and NsI_j^i represents the ith pixel of the jth block of *NsI*.

DnI is obtained using Equation (9):

$$DnI = \sum_{j=1}^{m} DnI_j^i \quad (9)$$

where *DnI* represents the combination of all the denoised block. The pixel weights are updated to the new grid of *DnI*. The proposed algorithm for the BD-based filtering technique in the MRI image is as follows:

Algorithm The proposed BD-based denoising algorithm

1 Input: *NsI & NrI* <-- Noisy & Normal MRI Images.
2 Consider Normal Image *NrI*.
3 Compute Noisy Image *NsI* by adding Noise to *NrI* using Equation (2).
4 Partition the Normal Image *NrI* into blocks and represent it using Equation (4).
5 Partition the Noise image *NsI* into blocks and represent it using Equation (6).
6 Find the Block difference BD between the blocks of Normal Image *NrI* Noisy image *NsI* using Equation (7).
7 If Block difference BD == 0 then
Update the pixel value of the block of the De-noised Image *DnI* using Equation (8).
Else if BD < 0 then
Update the pixel value of the block of the De-noised Image *DnI* using Equation (8).
Else if BD > 0 then
Update the pixel value of the block of the De-noised Image *DnI* using Equation (8).End if
8. End for
9. Output: *DnI*<-- De-noised MRI Image.

The next section gives the experimental result and discussion about the proposed BD-based filtering method.

4 | EXPERIMENTAL RESULTS AND DISCUSSION

The experimental analysis of the proposed method is estimated using the simulated MRI images from the BrainWeb database[19] and real patient images from the BraTS 2018 dataset. The BrainWeb dataset consists of 810 simulated MRI images with a different ratio of Rician noise of transverse, sagittal, and coronal modalities.[20] The different simulated MRI images are T1, T2, and PD weighted with several levels of Rician noises such as 3%, 6%, 9%, 12%, 15%, 18%, 21%, 24%, 27%, and 30%.[21] The normal and noisy (9% of Rician)-simulated MRI images are shown in Figure 2.

The proposed method is also estimated using real MRI images from the BraTS 2018 dataset.[22] From the dataset, about 160 real MRI images such as T1 and T2 with 9% of Rician noise are used for experimental analysis. The outcomes of the results for both the datasets are evaluated using metrics such as PSNR, structural similarity index measures (SSIM)**, universal quality index (UQI), and root mean square error (RMSE).[23]

The PSNR value is (qualitative measurement) calculated by using Equation (10):

$$\mathrm{PSNR} = 10\log 10\left(\frac{255^2}{\mathrm{MSE}}\right). \tag{10}$$

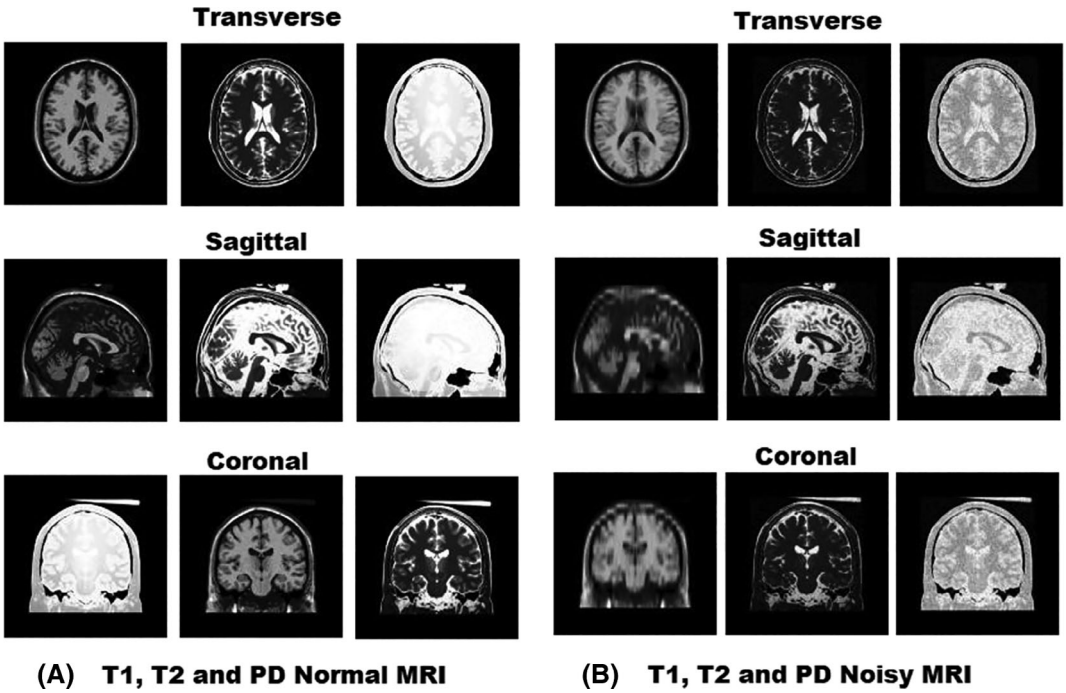

FIGURE 2 A, Normal and B, noisy T1-, T2-, and PD-simulated brain image portions shown at first, second, and third rows, respectively, with 9% Rician noise

MSE stands for the mean square error, which is calculated by using Equation (11):

$$\mathrm{MSE} = \frac{1}{mn}\sum_{i=0}^{mn-1}\left(d(i) - \hat{d}(i)\right)^2, \tag{11}$$

where $m \times n$ is the size of noise-free MRI image (d) and its noisy approximation ($\hat{d}$), and RMSE stands for root mean square error, which is calculated as the root value of MSE from Equation (11). The value of PSNR is measured in decibels (dB) and the large value as an identity of improved quality of denoised image.[24]

In UQI, the misrepresentation in an image is displayed as a combination of contrast and luminance; hence it is proved to be significant compared to other widely used misrepresentation metrics. The SSIM is for computing the similarity between two MRI images based on their data. The parameter of SSIM finds the similarity in a locality nearby pixel or batch by concatenating differences in correlation, average, and variance. The values of SSIM between two image blocks x and y from the denoised and normal images are calculated by using Equation (12):

$$\mathrm{SSIM}(x,y) = \frac{\left(2\mu_x\mu_y + C_1\right)\left(2\sigma_{xy} + C_2\right)}{\left(\mu_x^2 + \mu_y^2 + C_1\right)\left(\sigma_x^2 + \sigma_y^2 + C_2\right)}, \tag{12}$$

where μ_x and μ_y are the mean values of the blocks x and y, respectively, σ_x^2 and σ_y^2 are the variance of the blocks x and y, respectively, σ_{xy} is the covariance of the blocks x and y, C_1 and C_2 are the variables to stabilize the division with the weak denominator. The value of SSIM ranges in the interval [0-1], where the large value of SSIM pointed the better outcome of essential information.[25]

The residual image is the difference between the noise and the denoised image.[26] The residual image should not consist of functional structures as the happening of such structures denotes that the denoised image has missed useful edge and all-important information. On the other hand, the better operation of the denoised image might give the residual image that appears like degradation. The denoised and residual MRI images of the proposed method for the BrainWeb dataset are shown in Figure 3.

The performance analysis of the proposed method using PSNR, SSIM, UQI, and RMSE is shown in Tables 1 and 2 for the different percentages of Rician noise (3%-30%) of T1-weighted MRI images. From Tables 1 and 2, it is found that the proposed method shows better results than other existing methods. The proposed method obtains better SSIM value than all other existing methods.

Tables 3 and 4 show the PSNR, SSIM, UQI, and RMSE values for the T2-weighted MRI images. As analyzed from Tables 3 and 4, the proposed method shows the best results of PSNR, SSIM, UQI, and RMSE. The median filter gives the better PSNR values with low noise level than bilateral and anisotropic methods. Yet, for various levels of Rician noise, the proposed method gives a better performance outcome than other existing techniques.

Tables 5 and 6 show the performance metric values (PSNR, SSIM, UQI, and RMSE) of PD-weighted brain MRI images. As analyzed from Tables 5 and 6, the median filter

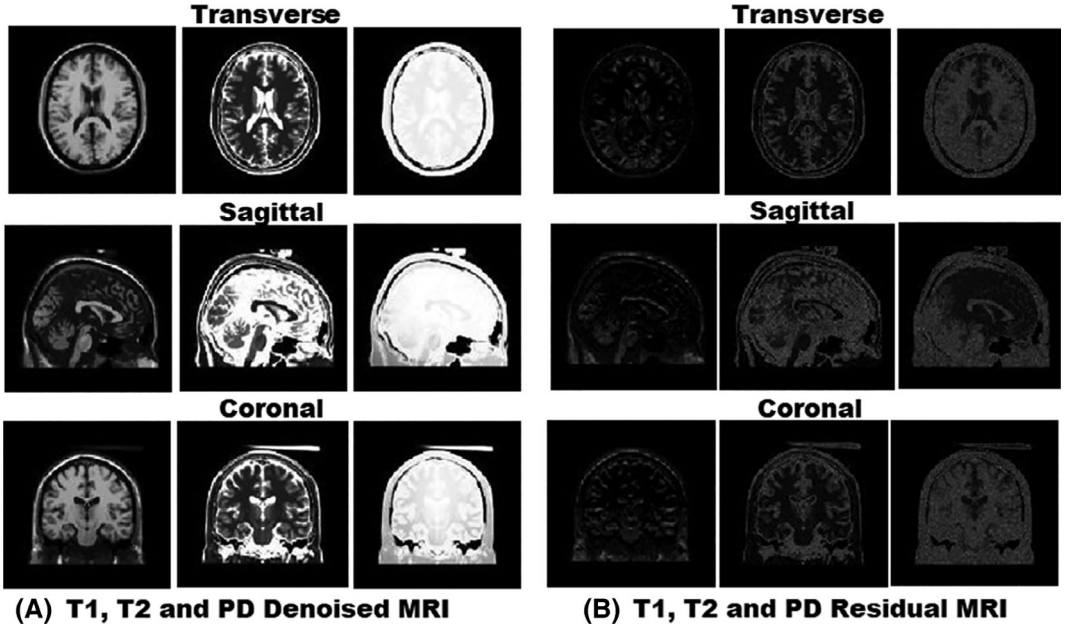

FIGURE 3 Results of the proposed method: A, denoised and B, residual images for simulated T1, T2, and PD brain images

TABLE 1 A comparative study of different existing methods with the proposed method based on the performance metrics of PSNR and SSIM for T1-weighted simulated MR images

	PSNR										SSIM									
Methods	**3%**	**6%**	**9%**	**12%**	**15%**	**18%**	**21%**	**24%**	**27%**	**30%**	**3%**	**6%**	**9%**	**12%**	**15%**	**18%**	**21%**	**24%**	**27%**	**30%**
Median[7]	40.87	36.58	33.84	32.15	30.71	30.51	30.23	30.05	29.78	29.54	0.9836	0.9661	0.9439	0.9176	0.8669	0.8649	0.8629	0.8609	0.8589	0.8569
Bilateral[8]	37.41	32.19	29.54	27.84	26.24	26.05	25.78	25.36	25.01	24.56	0.8968	0.7864	0.7303	0.6641	0.5994	0.5974	0.5954	0.5934	0.5914	0.5894
Anisotropic[9]	40.97	36.57	33.74	31.96	30.53	30.16	30.09	29.13	28.67	28.13	0.9837	0.9639	0.9401	0.9131	0.8645	0.8625	0.8605	0.8585	0.8565	0.8545
NLM[10]	39.65	36.93	33.98	32.06	30.89	30.57	30.09	29.64	29.57	29.13	0.9844	0.9648	0.9432	0.9167	0.8688	0.8668	0.8648	0.8628	0.8608	0.8588
IBLF[14]	40.26	37.01	34.03	32.26	30.98	30.23	30.14	29.79	29.67	29.45	0.9849	0.9655	0.9462	0.9189	0.8695	0.8675	0.8655	0.8635	0.8615	0.8595
WBNLM[13]	41.36	37.16	34.37	32.55	31.01	30.86	30.49	30.11	29.96	29.75	0.9853	0.9685	0.9474	0.9203	0.8714	0.8694	0.8674	0.8654	0.8634	0.8614
SANLM[15]	43.09	39.08	36.1	34.28	31.75	31.18	30.89	30.55	30.23	29.87	0.9815	0.9782	0.9523	0.9652	0.9701	0.9681	0.9661	0.9641	0.9621	0.9601
Proposed	45.94	46.65	39.06	34.73	31.79	31.56	31.23	30.98	30.54	30.16	0.9956	0.9866	0.9672	0.9704	0.9771	0.9751	0.9731	0.9711	0.9691	0.9671

Abbreviations: IBLF, Iterative Bilateral Filter; NLM, nonlocal mean filter; PSNR, peak signal-to-noise ratio; SANLM, spatial adaptive nonlocal mean; SSIM, structural similarity index measures; WBNLM, wavelet-based NLM.

TABLE 2 A comparative study of different existing methods with the proposed method based on the performance metrics of UQI and RMSE for T1-weighted simulated MR images

	UQI										RMSE									
Methods	**3%**	**6%**	**9%**	**12%**	**15%**	**18%**	**21%**	**24%**	**27%**	**30%**	**3%**	**6%**	**9%**	**12%**	**15%**	**18%**	**21%**	**24%**	**27%**	**30%**
Median[7]	0.9847	0.9671	0.9449	0.9186	0.8679	0.8659	0.8639	0.8619	0.8599	0.8579	2.5777	2.5807	2.5827	2.5867	2.5897	2.5927	2.5957	2.5987	2.6017	2.6047
Bilateral[8]	0.8979	0.7874	0.7313	0.6651	0.6004	0.5984	0.5964	0.5944	0.5924	0.5904	1.8682	1.8712	1.8732	1.8772	1.8802	1.8832	1.8862	1.8892	1.8922	1.8952
Anisotropic[9]	0.9848	0.9649	0.9411	0.9141	0.8655	0.8635	0.8615	0.8595	0.8575	0.8555	2.4741	2.4771	2.4791	2.4831	2.4861	2.4891	2.4921	2.4951	2.4981	2.5011
NLM[10]	0.9855	0.9658	0.9442	0.9177	0.8698	0.8678	0.8658	0.8638	0.8618	0.8598	1.9121	1.9151	1.9171	1.9211	1.9241	1.9271	1.9301	1.9331	1.9361	1.9391
IBLF[14]	0.986	0.9665	0.9472	0.9199	0.8705	0.8685	0.8665	0.8645	0.8625	0.8605	1.7315	1.7346	1.7465	1.7656	1.7523	1.7553	1.7583	1.7613	1.7643	1.7673
WBNLM[13]	0.9864	0.9695	0.9484	0.9213	0.8724	0.8704	0.8684	0.8664	0.8644	0.8624	1.6422	1.6452	1.6472	1.6512	1.6542	1.6572	1.6602	1.6632	1.6662	1.6692
SANLM[15]	0.9826	0.9792	0.9533	0.9662	0.9711	0.9691	0.9671	0.9651	0.9631	0.9611	1.5982	1.6012	1.6032	1.6072	1.6102	1.6132	1.6162	1.6192	1.6222	1.6252
Proposed	0.9967	0.9876	0.9682	0.9714	0.9781	0.9761	0.9741	0.9721	0.9701	0.9681	1.499	1.502	1.504	1.508	1.511	1.514	1.517	1.52	1.523	1.526

Abbreviations: IBLF, Iterative Bilateral Filter; NLM, nonlocal mean filter; RMSE, root mean square error; SANLM, spatial adaptive nonlocal mean; UQI, universal quality index; WBNLM, wavelet-based NLM.

TABLE 3 A comparative study of different existing methods with the proposed method based on the performance metrics of PSNR and SSIM for T2-weighted simulated MR images

	PSNR										SSIM									
Methods	**3%**	**6%**	**9%**	**12%**	**15%**	**18%**	**21%**	**24%**	**27%**	**30%**	**3%**	**6%**	**9%**	**12%**	**15%**	**18%**	**21%**	**24%**	**27%**	**30%**
Median[7]	35.73	31.66	29.31	27.64	25.88	24.12	23.07	22.06	21.06	20.19	0.9394	0.8983	0.8518	0.8165	0.7648	0.7618	0.7588	0.7558	0.7528	0.7498
Bilateral[8]	31.13	27.05	25.15	23.38	21.91	20.15	19.1	18.09	17.09	16.22	0.7842	0.6742	0.5931	0.5116	0.4529	0.4499	0.4469	0.4439	0.4409	0.4379
Anisotropic[9]	35.45	31.56	29.03	27.08	25.12	23.36	22.31	21.3	20.3	19.43	0.9266	0.8737	0.8308	0.7736	0.7221	0.7191	0.7161	0.7131	0.7101	0.7071
NLM[10]	36.02	31.96	29.17	27.56	25.46	23.7	22.65	21.64	20.64	19.77	0.9406	0.9077	0.8416	0.8023	0.7654	0.7624	0.7594	0.7564	0.7534	0.7504
IBLF[14]	36.12	31.98	29.36	27.66	25.59	23.83	22.78	21.77	20.77	19.9	0.9412	0.9046	0.8459	0.8124	0.7695	0.7665	0.7635	0.7605	0.7575	0.7545
WBNLM[13]	36.18	32.03	29.48	27.71	25.96	24.2	23.15	22.14	21.14	20.27	0.9443	0.9036	0.8528	0.8196	0.7774	0.7744	0.7714	0.7684	0.7654	0.7624
SANLM[15]	42.86	38.69	35.45	34.02	31.86	30.1	29.05	28.04	27.04	26.17	0.9865	0.9768	0.9626	0.9431	0.9265	0.9235	0.9205	0.9175	0.9145	0.9115
Proposed	45.83	45.25	44.97	43.39	41.91	40.15	39.1	38.09	37.09	36.22	0.9969	0.9951	0.9857	0.9568	0.9315	0.9285	0.9255	0.9225	0.9195	0.9165

Abbreviations: IBLF, Iterative Bilateral Filter; NLM, nonlocal mean filter; PSNR, peak signal-to-noise ratio; SANLM, spatial adaptive nonlocal mean; SSIM, structural similarity index measures; WBNLM, wavelet-based NLM.

TABLE 4 A comparative study of different existing methods with the proposed method based on the performance metrics of UQI and RMSE for T2-weighted simulated MR images

	UQI										RMSE									
Methods	**3%**	**6%**	**9%**	**12%**	**15%**	**18%**	**21%**	**24%**	**27%**	**30%**	**3%**	**6%**	**9%**	**12%**	**15%**	**18%**	**21%**	**24%**	**27%**	**30%**
Median[7]	0.9395	0.9315	0.9235	0.9155	0.9075	0.8995	0.8915	0.8835	0.8755	0.8675	2.5314	2.5236	2.5266	2.5296	2.5326	2.5346	2.5366	2.5386	2.5406	2.5426
Bilateral[8]	0.7843	0.7763	0.7683	0.7603	0.7523	0.7443	0.7363	0.7283	0.7203	0.7123	1.2119	1.2041	1.2071	1.2101	1.2131	1.2151	1.2171	1.2191	1.2211	1.2231
Anisotropic[9]	0.9267	0.9187	0.9107	0.9027	0.8947	0.8867	0.8787	0.8707	0.8627	0.8547	2.4953	2.4875	2.4905	2.4935	2.4965	2.4985	2.5005	2.5025	2.5045	2.5065
NLM[10]	0.9407	0.9327	0.9247	0.9167	0.9087	0.9007	0.8927	0.8847	0.8767	0.8687	1.8642	1.8564	1.8594	1.8624	1.8654	1.8674	1.8694	1.8714	1.8734	1.8754
IBLF[14]	0.9413	0.9333	0.9253	0.9173	0.9093	0.9013	0.8933	0.8853	0.8773	0.8693	1.7465	1.7325	1.7316	1.7319	1.7332	1.7352	1.7372	1.7392	1.7412	1.7432
WBNLM[13]	0.9444	0.9364	0.9284	0.9204	0.9124	0.9044	0.8964	0.8884	0.8804	0.8724	1.6111	1.6033	1.6063	1.6093	1.6123	1.6143	1.6163	1.6183	1.6203	1.6223
SANLM[15]	0.9866	0.9786	0.9706	0.9626	0.9546	0.9466	0.9386	0.9306	0.9226	0.9146	1.5909	1.5831	1.5861	1.5891	1.5921	1.5941	1.5961	1.5981	1.6001	1.6021
Proposed	0.997	0.989	0.981	0.973	0.965	0.957	0.949	0.941	0.933	0.925	1.4051	1.3973	1.4003	1.4033	1.4063	1.4083	1.4103	1.4123	1.4143	1.4163

Abbreviations: IBLF, Iterative Bilateral Filter; NLM, nonlocal mean filter; RMSE, root mean square error; SANLM, spatial adaptive nonlocal mean; UQI, universal quality index; WBNLM, wavelet-based NLM.

TABLE 5 A comparative study of different existing with the proposed method based on the performance metrics PSNR and SSIM for PD-weighted simulated MR images

	PSNR										SSIM									
Methods	**3%**	**6%**	**9%**	**12%**	**15%**	**18%**	**21%**	**24%**	**27%**	**30%**	**3%**	**6%**	**9%**	**12%**	**15%**	**18%**	**21%**	**24%**	**27%**	**30%**
Median[7]	35.73	31.66	29.31	27.64	25.88	24.72	23.56	22.4	21.24	20.08	0.9394	0.8983	0.8518	0.8165	0.7648	0.7618	0.7588	0.7558	0.7528	0.7498
Bilateral[8]	31.13	27.05	25.15	23.38	21.91	20.75	19.59	18.43	17.27	16.11	0.7842	0.6742	0.5931	0.5116	0.4529	0.4499	0.4469	0.4439	0.4409	0.4379
Anisotropic[9]	35.45	31.56	29.03	27.08	25.12	23.96	22.8	21.64	20.48	19.32	0.9266	0.8737	0.8308	0.7736	0.7221	0.7191	0.7161	0.7131	0.7101	0.7071
NLM[10]	36.05	31.96	29.55	27.65	25.46	24.3	23.14	21.98	20.82	19.66	0.9326	0.9011	0.8436	0.8028	0.7659	0.7629	0.7599	0.7569	0.7539	0.7509
IBLF[14]	36.1	31.99	29.68	27.69	25.62	24.46	23.3	22.14	20.98	19.82	0.9364	0.9026	0.8462	0.8078	0.7691	0.7661	0.7631	0.7601	0.7571	0.7541
WBNLM[13]	36.18	32.03	29.48	27.71	25.96	24.8	23.64	22.48	21.32	20.16	0.9443	0.9036	0.8528	0.8196	0.7774	0.7744	0.7714	0.7684	0.7654	0.7624
SANLM[15]	39.15	34.26	38.16	38.01	37.16	36	34.84	33.68	32.52	31.36	0.9786	0.9861	0.9645	0.9539	0.9218	0.9188	0.9158	0.9128	0.9098	0.9068
Proposed	48.17	46.91	46.47	45.15	42.41	41.25	40.09	38.93	37.77	36.61	0.9973	0.9952	0.9808	0.9601	0.9307	0.9277	0.9247	0.9217	0.9187	0.9157

Abbreviations: IBLF, Iterative Bilateral Filter; NLM, nonlocal mean filter; PSNR, peak signal-to-noise ratio; SANLM, spatial adaptive nonlocal mean; SSIM, structural similarity index measures; WBNLM, wavelet-based NLM.

TABLE 6 A comparative study of different existing methods with the proposed method based on the performance metrics of UQI and RMSE for PD-weighted simulated MR images

	UQI										RMSE									
Methods	**3%**	**6%**	**9%**	**12%**	**15%**	**18%**	**21%**	**24%**	**27%**	**30%**	**3%**	**6%**	**9%**	**12%**	**15%**	**18%**	**21%**	**24%**	**27%**	**30%**
Median[7]	0.9404	0.8993	0.8538	0.8185	0.7668	0.7648	0.7628	0.7608	0.7588	0.7568	2.1631	2.1553	2.1583	2.1613	2.1643	2.1663	2.1683	2.1703	2.1723	2.1743
Bilateral[8]	0.7852	0.6752	0.5951	0.5136	0.4549	0.4529	0.4509	0.4489	0.4469	0.4449	0.8309	0.8231	0.8261	0.8291	0.8321	0.8341	0.8361	0.8381	0.8401	0.8421
Anisotropic[9]	0.9276	0.8747	0.8328	0.7756	0.7241	0.7221	0.7201	0.7181	0.7161	0.7141	2.4804	2.4726	2.4756	2.4786	2.4816	2.4836	2.4856	2.4876	2.4896	2.4916
NLM[10]	0.9336	0.9021	0.8456	0.8048	0.7679	0.7659	0.7639	0.7619	0.7599	0.7579	1.7303	1.7225	1.7255	1.7285	1.7315	1.7335	1.7355	1.7375	1.7395	1.7415
IBLF[14]	0.9374	0.9036	0.8482	0.8098	0.7711	0.7691	0.7671	0.7651	0.7631	0.7611	1.7141	1.7156	1.7163	1.7175	1.7196	1.7216	1.7236	1.7256	1.7276	1.7296
WBNLM[13]	0.9453	0.9046	0.8548	0.8216	0.7794	0.7774	0.7754	0.7734	0.7714	0.7694	1.6812	1.6734	1.6764	1.6794	1.6824	1.6844	1.6864	1.6884	1.6904	1.6924
SANLM[15]	0.9796	0.9871	0.9665	0.9559	0.9238	0.9218	0.9198	0.9178	0.9158	0.9138	1.5268	1.519	1.522	1.525	1.528	1.53	1.532	1.534	1.536	1.538
Proposed	0.9983	0.9962	0.9828	0.9621	0.9327	0.9307	0.9287	0.9267	0.9247	0.9227	1.3694	1.3616	1.3646	1.3676	1.3706	1.3726	1.3746	1.3766	1.3786	1.3806

Abbreviations: IBLF, Iterative Bilateral Filter; NLM, nonlocal mean filter; RMSE, root mean square error; SANLM, spatial adaptive nonlocal mean; UQI, universal quality index; WBNLM, wavelet-based NLM.

TABLE 7 A comparative study of different existing methods with the proposed method based on performance metrics of PSNR and SSIM for T1-weighted real clinical MR images

	PSNR										SSIM									
Methods	**3%**	**6%**	**9%**	**12%**	**15%**	**18%**	**21%**	**24%**	**27%**	**30%**	**3%**	**6%**	**9%**	**12%**	**15%**	**18%**	**21%**	**24%**	**27%**	**30%**
Median[7]	38.97	34.68	31.94	30.25	29.234	28.2325	27.2311	26.2181	25.2169	24.2157	0.9806	0.9631	0.9409	0.9146	0.8639	0.8533	0.8428	0.8324	0.822	0.8117
Bilateral[8]	35.51	30.29	27.64	25.94	24.924	23.9225	22.9085	21.8955	20.8943	19.8931	0.8938	0.7834	0.7273	0.6611	0.5964	0.5858	0.5753	0.5649	0.5545	0.5442
Anisotropic[9]	39.07	34.67	31.84	30.06	29.044	28.0425	27.0285	26.0155	25.0143	24.0131	0.9807	0.9609	0.9371	0.9101	0.8615	0.8509	0.8404	0.83	0.8196	0.8093
NLM[10]	37.75	35.03	32.08	30.16	29.144	28.1425	27.1285	26.1155	25.1143	24.1131	0.9814	0.9618	0.9402	0.9137	0.8658	0.8552	0.8447	0.8343	0.8239	0.8136
IBLF[14]	38.15	35.12	32.24	30.41	29.394	28.3925	27.3785	26.3655	25.3643	24.3631	0.9819	0.9645	0.9431	0.9162	0.8663	0.8557	0.8452	0.8348	0.8244	0.8141
WBNLM[13]	39.46	35.26	32.47	30.65	29.634	28.6325	27.6185	26.6055	25.6043	24.6031	0.9823	0.9655	0.9444	0.9173	0.8684	0.8578	0.8473	0.8369	0.8265	0.8162
SANLM[15]	41.19	37.18	34.2	32.38	31.364	30.3625	29.3485	28.3355	27.3343	26.3331	0.9785	0.9752	0.9493	0.9622	0.9671	0.9565	0.946	0.9356	0.9252	0.9149
Proposed	44.04	44.75	37.16	32.83	31.814	30.8125	29.7985	28.7855	27.7843	26.7831	0.9926	0.9836	0.9642	0.9674	0.9741	0.9635	0.953	0.9426	0.9322	0.9219

Abbreviations: IBLF, Iterative Bilateral Filter; NLM, nonlocal mean filter; PSNR, peak signal-to-noise ratio; SANLM, spatial adaptive nonlocal mean; SSIM, structural similarity index measures; WBNLM, wavelet-based NLM.

TABLE 8 A comparative study of different existing methods with the proposed method based on performance metrics of UQI and RMSE for T1-weighted real clinical MR images

	UQI										RMSE									
Methods	**3%**	**6%**	**9%**	**12%**	**15%**	**18%**	**21%**	**24%**	**27%**	**30%**	**3%**	**6%**	**9%**	**12%**	**15%**	**18%**	**21%**	**24%**	**27%**	**30%**
Median[7]	0.986	0.9685	0.9463	0.92	0.8693	0.8587	0.8482	0.8378	0.8274	0.8171	2.6377	2.6407	2.6427	2.6467	2.6497	2.6522	2.6547	2.6572	2.6597	2.6622
Bilateral[8]	0.8992	0.7888	0.7327	0.6665	0.6018	0.5912	0.5807	0.5703	0.5599	0.5496	1.9282	1.9312	1.9332	1.9372	1.9402	1.9427	1.9452	1.9477	1.9502	1.9527
Anisotropic[9]	0.9861	0.9663	0.9425	0.9155	0.8669	0.8563	0.8458	0.8354	0.825	0.8147	2.5341	2.5371	2.5391	2.5431	2.5461	2.5486	2.5511	2.5536	2.5561	2.5586
NLM[10]	0.9868	0.9672	0.9456	0.9191	0.8712	0.8606	0.8501	0.8397	0.8293	0.819	1.9721	1.9751	1.9771	1.9811	1.9841	1.9866	1.9891	1.9916	1.9941	1.9966
IBLF[14]	0.9873	0.9699	0.9485	0.9216	0.8717	0.8611	0.8506	0.8402	0.8298	0.8195	1.8652	1.8664	1.8695	1.8731	1.8759	1.8784	1.8809	1.8834	1.8859	1.8884
WBNLM[13]	0.9877	0.9709	0.9498	0.9227	0.8738	0.8632	0.8527	0.8423	0.8319	0.8216	1.7022	1.7052	1.7072	1.7112	1.7142	1.7167	1.7192	1.7217	1.7242	1.7267
SANLM[15]	0.9839	0.9806	0.9547	0.9676	0.9725	0.9619	0.9514	0.941	0.9306	0.9203	1.6582	1.6612	1.6632	1.6672	1.6702	1.6727	1.6752	1.6777	1.6802	1.6827
Proposed	0.998	0.989	0.9696	0.9728	0.9795	0.9689	0.9584	0.948	0.9376	0.9273	1.5591	1.5621	1.5641	1.5681	1.5711	1.5736	1.5761	1.5786	1.5811	1.5836

Abbreviations: IBLF, Iterative Bilateral Filter; NLM, nonlocal mean filter; RMSE, root mean square error; SANLM, spatial adaptive nonlocal mean; UQI, universal quality index; WBNLM, wavelet-based NLM.

TABLE 9 A comparative study of different existing methods with the proposed method based on performance metrics of PSNR and SSIM for T2-weighted real clinical MR images

	PSNR										SSIM									
Methods	**3%**	**6%**	**9%**	**12%**	**15%**	**18%**	**21%**	**24%**	**27%**	**30%**	**3%**	**6%**	**9%**	**12%**	**15%**	**18%**	**21%**	**24%**	**27%**	**30%**
Median[7]	33.83	29.76	27.41	25.74	23.98	22.83	21.43	20.3	19.18	18.07	0.9364	0.8953	0.8488	0.8135	0.7618	0.9364	0.8953	0.8488	0.8135	0.7618
Bilateral[8]	29.23	25.15	23.25	21.48	20.01	18.86	17.46	16.33	15.21	14.1	0.7812	0.6712	0.5901	0.5086	0.4499	0.7812	0.6712	0.5901	0.5086	0.4499
Anisotropic[9]	33.55	29.66	27.13	25.18	23.22	22.07	20.67	19.54	18.42	17.31	0.9236	0.8707	0.8278	0.7706	0.7191	0.9236	0.8707	0.8278	0.7706	0.7191
NLM[10]	34.12	30.06	27.17	25.66	23.56	22.41	21.01	19.88	18.76	17.65	0.9376	0.9047	0.8386	0.7991	0.7624	0.9376	0.9047	0.8386	0.7991	0.7624
IBLF[14]	34.19	30.09	27.36	25.72	23.91	22.76	21.36	20.23	19.11	18	0.9396	0.9215	0.8402	0.8052	0.7687	0.9396	0.9215	0.8402	0.8052	0.7687
WBNLM[13]	34.28	30.13	27.58	25.81	24.06	22.91	21.51	20.38	19.26	18.15	0.9413	0.9306	0.8498	0.8166	0.7744	0.9413	0.9306	0.8498	0.8166	0.7744
SANLM[15]	40.96	36.79	33.55	32.12	29.96	28.81	27.41	26.28	25.16	24.05	0.9835	0.9738	0.9596	0.9401	0.9235	0.9835	0.9738	0.9596	0.9401	0.9235
Proposed	43.93	43.35	43.07	41.49	40.01	38.86	37.46	36.33	35.21	34.1	0.9939	0.9921	0.9827	0.9538	0.9285	0.9939	0.9921	0.9827	0.9538	0.9285

Abbreviations: IBLF, Iterative Bilateral Filter; NLM, nonlocal mean filter; PSNR, peak signal-to-noise ratio; SANLM, spatial adaptive nonlocal mean; SSIM, structural similarity index measures; WBNLM, wavelet-based NLM.

TABLE 10 A comparative study of different existing methods with the proposed method based on performance metrics of UQI and RMSE for T2-weighted real clinical MR images

	UQI										RMSE									
Methods	**3%**	**6%**	**9%**	**12%**	**15%**	**18%**	**21%**	**24%**	**27%**	**30%**	**3%**	**6%**	**9%**	**12%**	**15%**	**18%**	**21%**	**24%**	**27%**	**30%**
Median[7]	0.9394	0.8983	0.8518	0.8165	0.7648	0.9394	0.8983	0.8518	0.8165	0.7648	2.5914	2.5836	2.5866	2.5896	2.5926	2.5956	2.5986	2.6016	2.6046	2.6076
Bilateral[8]	0.7842	0.6742	0.5931	0.5116	0.4529	0.7842	0.6742	0.5931	0.5116	0.4529	1.2719	1.2641	1.2671	1.2701	1.2731	1.2761	1.2791	1.2821	1.2851	1.2881
Anisotropic[9]	0.9266	0.8737	0.8308	0.7736	0.7221	0.9266	0.8737	0.8308	0.7736	0.7221	2.5553	2.5475	2.5505	2.5535	2.5565	2.5595	2.5625	2.5655	2.5685	2.5715
NLM[10]	0.9406	0.9077	0.8416	0.8021	0.7654	0.9406	0.9077	0.8416	0.8021	0.7654	1.9242	1.9164	1.9194	1.9224	1.9254	1.9284	1.9314	1.9344	1.9374	1.9404
IBLF[14]	0.9426	0.9245	0.8432	0.8082	0.7717	0.9426	0.9245	0.8432	0.8082	0.7717	1.8615	1.8523	1.8429	1.8456	1.8498	1.8528	1.8558	1.8588	1.8618	1.8648
WBNLM[13]	0.9443	0.9336	0.8528	0.8196	0.7774	0.9443	0.9336	0.8528	0.8196	0.7774	1.6711	1.6633	1.6663	1.6693	1.6723	1.6753	1.6783	1.6813	1.6843	1.6873
SANLM[15]	0.9865	0.9768	0.9626	0.9431	0.9265	0.9865	0.9768	0.9626	0.9431	0.9265	1.6509	1.6431	1.6461	1.6491	1.6521	1.6551	1.6581	1.6611	1.6641	1.6671
Proposed	0.9969	0.9951	0.9857	0.9568	0.9315	0.9969	0.9951	0.9857	0.9568	0.9315	1.4651	1.4573	1.4603	1.4633	1.4663	1.4693	1.4723	1.4753	1.4783	1.4813

Abbreviations: IBLF, Iterative Bilateral Filter; NLM, nonlocal mean filter; RMSE, root mean square error; SANLM, spatial adaptive nonlocal mean; UQI, universal quality index; WBNLM, wavelet-based NLM.

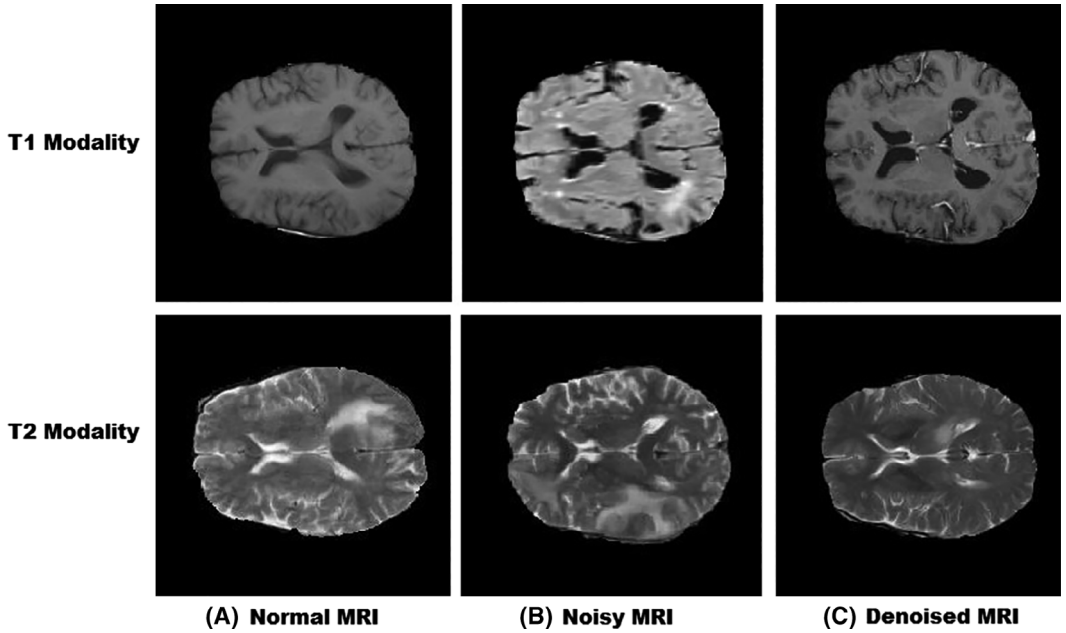

FIGURE 4 Results of real clinical MRI brain images: A, normal, B, noisy, and C, denoised for T1 and T2 images

gives better PSNR and SSIM values than other methods such as bilateral and anisotropic methods. Yet the proposed method gives high PSNR, SSIM, UQI, and RMSE values compared to other existing techniques.

Tables 7 and 8 shows the performance metric values of T1-weighted real clinical limited MRI images taken from the BraTS dataset. As analyzed from Tables 7 and 8, the proposed method gives better values of performance. Tables 9 and 10 show T2-weighted real clinical limited MRI images. The proposed method yields the best outcome result compared with other existing denoising methods in Tables 9 and 10. The normal, noisy, and denoised real MRI images of the proposed method for the BraTS dataset are presented in Figure 4.

In the experimental results, the state-of-the-art methods for denoising MRI images such as median, bilateral, ADF, and NLM techniques and recent denoising techniques such as IBLF, WBNLM, and SANLM techniques were compared with the proposed method. Median filter eliminates most of the noise from the MRI images. However, it removes the details of the minute structure. The bilateral filter gives a more honest resolution but raises the miserable character of an image to remove noise in the low-frequency region of the MRI image.[27] The anisotropic filter decreases the noise but fails to keep fine edges.[28] NLM overcomes the restrictions of all other existing methods, but the execution time is more than other existing techniques. In IBLF, the bias correction is done before each operation to get the denoised MRI image, and the bias correction is reestimated after each iteration. Only the noise ratio is increased, but the performance metric values are decreased accordingly. In WBNLM, the scaling coefficient is not modified and it is typically estimated by wavelet shrinkage. This may lead to image discontinuity. Therefore, the main drawback of this method is before applying NLM techniques, the pre-stage convention method is applied in the noisy image. In SANLM, when dealing with nonstationary noise, the use of a global noise variance across the image will lead to suboptimal outcomes. The proposed method overcomes the drawback of all other existing denoising techniques and also got the best outcome based on the performance metrics such as PSNR, SSIM, UQI, and RMSE.

TABLE 11 Comparison of the execution time of the proposed work with existing works

	Average elapsed time (in seconds)–simulated MRI BrainWeb dataset (810 Nos)		
Methods	**T1 weighted**	**T2 weighted**	**PD weighted**
Median[7]	32.85	12.43	11.7
Bilateral[8]	39.42	14.91	14.04
Anisotropic[9]	45.99	17.4	16.38
NLM[10]	68.16	26.49	24.99
IBLF[14]	66.34	25.19	24.55
WBNLM[13]	65.74	24.86	23.41
SANLM[15]	30.65	15.47	12.29
Proposed	26.28	9.945	9.366

Abbreviations: IBLF, Iterative Bilateral Filter; NLM, nonlocal mean filter; SANLM, spatial adaptive nonlocal mean; WBNLM, wavelet-based NLM.

The proposed method reduces the noise at maximum and also maintains the finest limits and structure, thus preserving the significant information of MRI images. Table 11 shows the execution time of existing denoising methods with the proposed method. The execution time of the proposed

method is really less than the SANLM techniques because the proposed method focuses on the block-based noise difference approach to denoise the MRI images. Hence, the proposed method yields a more beneficial effect than other existing approaches.

5 | CONCLUSION AND FUTURE WORK

The proposed method represents the removal of noise in MRI image using the block difference-based filtering technique. The proposed method provides more reliable performance in reducing the noise, because the proposed method deals with an efficient manipulation of each and every pixel weight and the further split of edge pixels from the noise pixels. Thus, the proposed method produces a better result compared to other existing methods. The method is also evaluated on transverse, sagittal, and coronal views of T1, T2, and PD modality of simulated MRI images and T1 and T2 real MRI images. In the future, the same method can be extended to compute the execution time of real clinical patient MRI images, and focus will also be on the improvement in the accuracy of the proposed method using an angular rotation-based block difference technique.

ORCID

G.G. Lakshmi Priya https://orcid.org/0000-0001-5322-1518

REFERENCES

1. Aja-Fernandez S, Alberola-López C, Westin C-F. Noise and signal estimation in magnitude MRI and Rician distributed images: a LMMSE approach. *IEEE Trans Image Process*. 2008;17(8):1383-1398.
2. Buades A, Coll B, Morel JM. A review of image denoising algorithms, with a new one. *Multiscale Model Sim*. 2005;4(2): 490-530.
3. Punhani P, Garg NK, Noise removal in MR images using non-linear filters, IEEE, 6th ICCCNT. 2015.
4. Aarya I, Jiang D, Gale T. Signal-dependent Rician noise denoising using nonlinear filter. *Lect Notes Softw Eng*. 2013;1(4):344-349.
5. More S, Hanchate VV. A survey on magnetic resonance image denoising methods. *IRJET*. 2016;3(5):250–256.
6. Chandrashekar L, Sreedevi A, Assessment of non-linear filters for MRI images, IEEE, 2017 Second International Conference on Electrical, Computer and Communication Technologies (ICECCT). 978-1-5090-3239.
7. Rahmat R, Malik AS, Kamel N. Comparison of LULU and median filter for image de-noising. *Inter J Comput Elect Eng*. 2013;5(6):568-571.
8. Perona P, Malik J. Scale-space and edge detection using anisotropic diffusion. *IEEE Trans Pattern Anal Mach Intell*. 1990;12 (7):629-639.
9. Tomasi, C. Manduchi, R. Bilateral filtering for gray and color images, Presented at the 6th International Conference on Computer Vision, Bombay, India, 1998; 839–846.
10. Manjón JV, Thacker NA, Lull JJ, et al. MRI denoising using non-local means. *Med Image Anal*. 2008;31(12):514-523.
11. Bhujle HV, Vadavadagi BH. NLM based magnetic resonance image denoising – a review. *Biomed Signal Process Control*. 2018;47:252-261.
12. Manjón JV, Coupé P, Martí-Bonmatí L, Collins DL, Robles M. Adaptive nonlocal means denoising of MR images with spatially varying noise levels. *Magn Reson Imaging*. 2010;31:192-203.
13. Balachandar R, Rajkumar R. Efficient and robust denoising of magnetic resonance brain images based on wavelet-based nonlocal means algorithm. *Inter J Eng Sci*. 2015;13:84-89.
14. Kaur M, Kaur R. A comparative analysis of noise reduction filters in MRI images. *IRJET*. 2016;3(5):238-242.
15. Saritha Saladi N, Prabha A. Analysis of denoising filters on MRI brain images. *Int J Imaging Syst Technol*. 2017;27:201-208.
16. Mohana J, Krishnaveni V, Guo Y. Survey on the magnetic resonance image denoising methods. *Biomed Signal Process Control*. 2014;9(3):56-69.
17. Gudbjartsso H, Patz S. The Rician distribution of noisy MRI data. *Magn Reson Med*. 1995;34(6):910-914.
18. Wiest-Daesslé N, Prima S, Coupé P, Morrissey SP, Barillot C. Rician noise removal by non-local means filtering for low signal-to-noise ratio misapplications to DT-MRI. *Med Image Comput Assist Interv*. 2008;11:171-179.
19. Brain Web: Simulated Brain Database. Available online at: http://www.bic.mni.mcgill.ca/brainweb.
20. The Basics of MRI Image Modality. Available online at: http://casemed.case.edu/clerkships/neurology/web%20neurorad/mri%20basics.htm.
21. Samsonov A, Johnson C. Noise-adaptive nonlinear diffusion filtering of MR images with spatially varying noise levels. *Magn Reson Med*. 2004;52:798-806.
22. *BraTS*: Real clinical MRI Images Database. Available online at http://braintumorsegmentation.org/.
23. Redpath TW. Commentary signal-to-noise ratio in MRI. *Br J Radiol*. 1998;71:704-707.
24. Firbank M, Coulthard A, Harrison R, Williams E. A comparison of two methods for measuring the signal to noise ratio on MR images. *Phys Med Biol*. 1999;44(12):261.
25. Henkleman RM. Measurement of signal intensities in the presence of noise in MR images. *Med Phys*. 1985;12(2):232-243.
26. McVeigh ER, Henkelman RM, Bronskill MJ. Noise and filtration in magnetic resonance imaging. *Med Phys*. 1985;12:586-591.
27. Joseph J, Periyasamy R. an image driven bilateral filter with adaptive range and spatial parameters for denoising magnetic resonance images. *Comput Elect Eng*. 2018;69:782-795.
28. Baselice F, Ferraioli G, Pascazio V, Sorriso A. Bayesian MRI denoising in the complex domain. *Magn Reson Imaging*. 2017;38: 112-122.

How to cite this article: Nagarajan I, Lakshmi Priya GG. Removal of noise in MRI images using a block difference-based filtering approach. *Int J Imaging Syst Technol*. 2019;1–13. https://doi.org/10.1002/ima.22361